JOURNAL OF BACTERIOLOGY, Mar. 2007, p. 2331–2338 Vol. 189, No. 6
0021-9193/07/$08.00+0 doi:10.1128/JB.01656-06

Mutagenesis and Repair in *Bacillus anthracis*: the Effect of Mutators[▽]

Krystle Zeibell, Sharon Aguila, Vivian Yan Shi, Andrea Chan, Hanjing Yang, and Jeffrey H. Miller*

Department of Microbiology, Immunology, and Molecular Genetics, and The Molecular Biology Institute, University of California, Los Angeles, California 90095

Received 25 October 2006/Accepted 21 December 2006

We have generated mutator strains of *Bacillus anthracis* Sterne by using directed gene knockouts to investigate the effect of deleting genes involved in mismatch repair, oxidative repair, and maintaining triphosphate pools. The single-knockout strains are deleted for *mutS*, *mutY*, *mutM*, or *ndk*. We also made double-knockout strains that are *mutS ndk* or *mutY mutM*. We have measured the levels of mutations in the *rpoB* gene that lead to the Rif^r phenotype and have examined the mutational specificity. In addition, we examined the mutational specificity of two mutagens, 5-azacytidine and *N*-methyl-*N*′-nitro-*N*-nitroso-guanidine. The *mutY* and *mutM* single knockouts are weak mutators by themselves, but the combination of *mutY mutM* results in very high mutation rates, all due to G:C → T:A transversions. The situation parallels that seen in *Escherichia coli*. Also, *mutS* knockouts are strong mutators and even stronger in the presence of a deletion of *ndk*. The number of sites in *rpoB* that can result in the Rif^r phenotype by single-base substitution is more limited than in certain other bacteria, such as *E. coli* and *Deinococcus radiodurans*, although the average mutation rate per mutational site is roughly comparable. Hotspots at sites with virtually identical surrounding sequences are organism specific.

Mutational pathways, mutagenesis, and DNA repair systems are an integral part of biology. On the one hand, unchecked mutagenesis can lead to aberrant cellular physiology, cell death, and myriad human diseases, including cancer (for a review, see reference 8). On the other hand, mutational pathways can be a driving force in adaptive evolution, can create sufficient antigenic variation to allow pathogens to overcome host immune responses, and are instrumental in generating antibody diversity (for a review, see reference 19). Surprisingly, mutagenesis and repair have been studied in detail in only a very small number of organisms, such as *Escherichia coli* and *Salmonella*, yeast, and humans. As the field of genomics opens up possibilities for examining mutational pathways and repair strategies in a wide range of microorganisms, it is important to study these processes in microorganisms of interest. We will no doubt uncover many new mechanisms and will also learn more about the organism in question. In this study we focus on *Bacillus anthracis*, a bacterium of great interest for biodefense.

Bacillus anthracis is a gram-positive spore-forming bacillus that can infect humans, causing anthrax (for a review, see reference 15). Two plasmids are responsible for the virulence of *B. anthracis*. These are pXO1, which encodes the toxin protein and the lethal and edema factors, among other proteins (11, 24), and pXO2, encoding the capsule biosynthesis and depolymerization proteins, as well as additional factors (4, 10, 15, 30). The durable endospore and the lethality of inhalation anthrax make *B. anthracis* a powerful bioweapon. The complete 5.23-Mb sequence of the *B. anthracis* Ames genome has been determined, and it encodes 5,508 predicted protein-coding sequences (25). Annotation of the *B. anthracis* genome reveals 165 clusters of orthologous groups (COGs) in the category of DNA replication, recombination, and repair (http://www.ncbi.nlm.nih.gov/sutils/cogtik.cgi?gi=405&cog=L). The genome predicts the existence of an extra 53 proteins that are not present in its close relative *Bacillus subtilis* (http://www.ncbi.nlm.nih.gov/sutils/cogtik.cgi?gi=27&cog=L). *B. anthracis* has many of the DNA repair functions predicted for *B. subtilis*, as well as additional predicted repair functions, including repair proteins aimed at reversing UV-induced DNA damage and at reducing oxidative damage, such as bromoperoxidase, thiol-peroxidase, thioredoxin proteins, and a Cu-Zn superoxide dismutase (25). The latter is involved in the virulence of other bacteria, such as *Salmonella*, protecting them from nitric oxide killing (5). These findings underscore the need for examining mutational pathways and DNA repair in *B. anthracis* rather than just in *B. subtilis*. In any case, repair systems have essentially not been studied in *B. anthracis* and only sparingly in *B. subtilis* (see, however, references 27 and 28).

In this study we used directed gene knockouts to derive a set of mutator strains of *B. anthracis* deficient in mismatch repair, as well as oxidative repair, and characterize these strains with regard to mutation rates and mutational specificity. We also examine the specificity of several mutagens in this organism and extend the *rpoB*/Rif^r mutational analysis system that has been used with other bacteria (e.g., see references 9 and 14), as well as with *B. anthracis* (31), and use this system to measure mutation rates at specific sites.

MATERIALS AND METHODS

Bacterial strains, plasmids, media, antibiotics, and growth conditions. All of the *B. anthracis* strains used in this study are derivatives of the wild-type *B. anthracis* Sterne 7702, a gift from K. Bradley (University of California, Los Angeles). The plasmids pUTE618, pUTE619, and pUTE583 are gifts from T. M. Koehler (The University of Texas Health Science Center Medical School). Unless described elsewhere, bacterial cultures were grown in standard LB medium supplemented with kanamycin (100 μg/ml), spectinomycin (100 μg/ml), and erythromycin (5 μg/ml) when appropriate.

Construction of *B. anthracis* single- and double-knockout mutants. The procedure for making single- or double-knockout mutants is described in the text, in

* Corresponding author. Mailing address: Department of MIMG/UCLA, 1602 Molecular Sciences Bldg., 405 Hilgard Ave., Los Angeles, CA 90095. Phone: (310) 825-8460. Fax: (310) 206-3088. E-mail: jhmiller@microbio.ucla.edu.

▽ Published ahead of print on 12 January 2007.

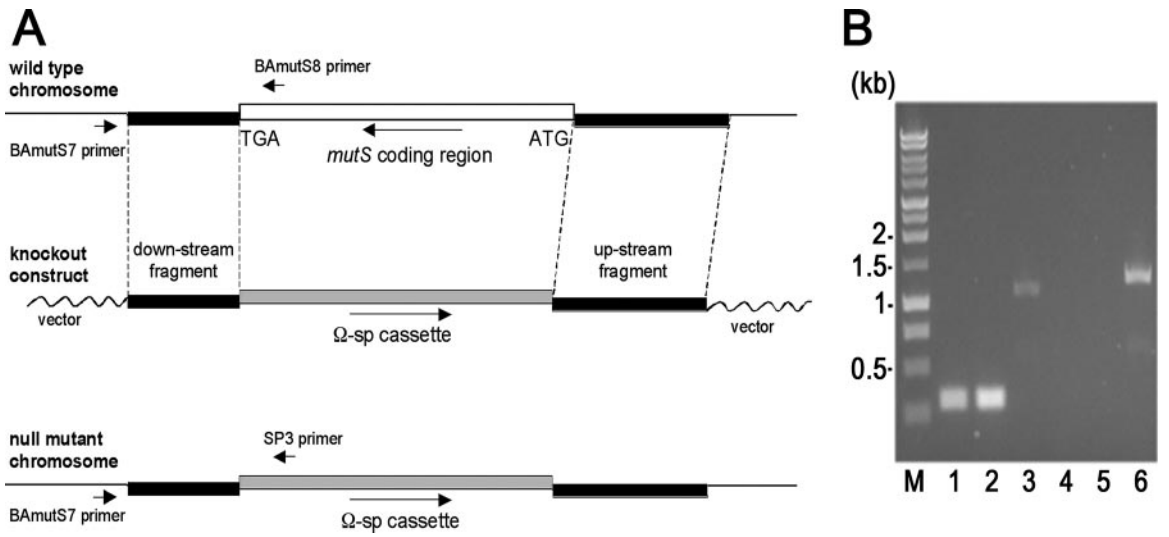

FIG. 1. Construction of a *B. anthracis mutS* knockout mutant. (A) Schematic representation of the targeting strategy for generating the *mutS* null allele. The *mutS* coding region was replaced by a spectinomycin resistance-encoding cassette through recombination of homologous flanking sequences. A white box represents the *mutS*-coding region. Black boxes represent homologous sequences flanking the *mutS* gene. Gray boxes represent the spectinomycin resistance-encoding cassette. (B) PCR analysis of genomic DNA isolated from the wild type (lanes 1, 3, and 5) and *mutS* knockout mutant (lanes 2, 4, and 6). Lanes 1 and 2, primers F1 and R1 for the *B. anthracis rpoB* gene (31); lanes 3 and 4, primers BAmutS7 and BAmutS8 (see panel A); lanes 5 and 6, primers BAmutS7 and SP3 (see panel A); lane M, 1-kb DNA ladder standard (sizes are marked to the left).

Fig. 1, and in Fig. 2. It was slightly modified from the protocol developed in the laboratory of Koehler, as described previously (3, 16, 26), to precisely replace an open reading frame (ORF) with an antibiotic resistance-encoding cassette. Typically, a 1-kb sequence immediately upstream of the ORF was amplified by PCR using primers that contain the restriction enzyme recognition sites BamHI and SalI. A 1-kb sequence immediately downstream of the ORF was amplified by PCR using primers that contain the restriction enzyme recognition sites SalI and SacI. Both PCR-amplified DNA fragments were cloned into pCR2.1TOPO vector with the TOPO TA cloning kit (Invitrogen). The cloned DNA fragments were verified by DNA sequencing, and the clones with compatible orientations were used to construct the plasmid connecting both the upstream and downstream fragments in the appropriate orientation at the SalI site. The antibiotic resistance-encoding cassette from either pUTE618 (Ω-Km) (3) or pUTE619 (Ω-Sp) (3) was inserted at the SalI site. The knockout construct that contains the upstream flanking region–antibiotic resistance-encoding cassette–downstream flanking region was isolated after SacI digestion and subcloned into the shuttle vector pUTE583 (3).

The protocols for preparing pUTE583 derivatives from a Dam$^-$ *E. coli* strain, electroporation into *B. anthracis*, and reciprocal recombination were as previously described (3, 16, 26). Each knockout mutant was verified by PCR, demonstrating the loss of the wild-type allele and the presence of the antibiotic resistance-encoding cassette. The sequences of the primers used in each knockout construction are available upon request.

Site-directed mutagenesis of the *B. anthracis rpoB* gene. The procedure for site-directed mutagenesis of the *rpoB* gene is described in the text and in Fig. 5.

Mutagenesis. 5-Azacytidine (5AZ) was used at a concentration of 100 μg/ml in LB, and MNNG (*N*-methyl-*N*′-nitro-*N*-nitrosoguanidine) was used at 100 μg/ml. For 5AZ, cells were grown overnight in LB from an inoculum of 100 to 1,000 cells (see also reference 9). For MNNG mutagenesis, the procedures are essentially as described previously (18).

Detection of mutants. Rif^r colonies were selected as described previously (9, 18). Briefly, overnight cultures were seeded with several hundred cells and grown overnight at 37°C on a rotor to provide aeration. Dilutions of the overnight cultures were plated on selective medium (LB containing 50 μg/ml rifampin) at 37°C to detect Rif^r colonies and on LB for determining the viable cell titer. For spontaneous mutants from a wild-type background, cells were concentrated before plating. Colonies were scored after 18 to 24 h. In order to avoid picking bias based on colony size, the colony closest to a target point in the center of each plate was picked in each case. Only the results from this colony appear in Table 2, although additional mutations were analyzed. Mutation frequencies were determined, and the median frequency (*f*) from a set of cultures (the number of cultures varied from 15 to 50) was used to calculate the mutation rate (μ) per replication, by the method of Drake (7), with the formula $\mu = f/\ln(N\mu)$ where N is the number of cells in the culture; 95% confidence limits were determined according to the method of Dixon and Massey (6).

DNA isolation. DNA was isolated directly from single colonies, as described previously by Keim and coworkers (12), with slight modifications in the resuspension volume (60 μl of Tris-EDTA buffer) and supernatant transfer volume (30 μl).

RESULTS

Construction of a set of DNA repair gene knockout mutants. We used the following procedure, as exemplified by the construction of a *mutS* knockout, shown in Fig. 1. A DNA construct for making a *mutS* null mutant by precise ORF replacement was engineered by a slightly modified procedure of Koehler and coworkers (3; also T. Koehler, personal communication). Briefly, a 1.2-kb upstream flanking region (starting before the *mutS* start codon) and a 0.9-kb downstream flanking region (starting after the *mutS* stop codon) were PCR amplified and cloned into separate pCR2.1 TOPO vectors (Invitrogen). Then, the downstream fragment was subcloned behind the upstream fragment, and subsequently a Ω-Sp DNA cassette, from the plasmid pUTE619, which confers spectinomycin resistance (Fig. 1A), was inserted between the two fragments.

The *mutS* knockout construct was then subcloned into a shuttle vector (pUTE583) that contains an erythromycin resistance determinant but is unstable in *B. anthracis* when grown in liquid medium without selection (3; also T. Koehler, personal communication). The DNA of the resulting *mutS* knockout construct, pUTE583Δ*mutS*, was prepared from a Dam$^-$ *E. coli* strain (GM2163) and electroporated into *B. anthracis* wild-type cells. Erythromycin-resistant transformants were selected and purified. To allow reciprocal recombination to take place and

TABLE 1. *B. anthracis* knockout mutants

Knockout constructed	Function
Single	
mutS (BAS3618)	DNA mismatch repair protein
mutY (BAS0491)	A/G-specific adenine glycosylase
mutM (BAS4481)	Formamidopyrimidine-DNA glycosylase
ndk (BAS1425)	Nucleoside diphosphate kinase
Double	
mutS ndk	
mutY mutM	

TABLE 2. *B. anthracis rpoB* mutation frequencies (f) and rates (μ)[a]

Genotype	f (10^a)	μ (10^a)[b]
Wild type	2.8 (1.7–4.7)	1.6 (1.2–2.3)
mutM	6.1 (2.8–8.9)	3.2 (2.0–4.1)
mutY	33 (31–56)	9.4 (9.0–14)
mutY mutM	2,800 (2,500–3,300)	430 (390–500)
ndk	8.0 (5.0–13)	3.7 (2.8–5.3)
mutS	500 (480–550)	87 (84–94)
mutS ndk	2,200 (1,500–4,800)	360 (260–710)

[a] Values in parentheses are 95% confidence limits (6).
[b] Mutation rates are calculated by the method of Drake (7).

a subsequent loss of the shuttle vector, the purified transformants were grown in liquid medium for several days without erythromycin. The *mutS* knockout mutants were identified as those colonies that were spectinomycin resistant but erythromycin sensitive. The disruption of the wild-type *mutS* allele generated by precise ORF replacement with the Ω-Sp cassette was verified by PCR, demonstrating the absence of the wild-type *mutS* allele with the primer pair BAmutS7 and BAmutS8 (Fig. 1B, lane 4; the locations of both primers are shown in Fig. 1A) and the presence of the Ω-Sp DNA cassette with the primer pair BAmutS7 and SP3 (Fig. 1B, lane 6; the locations of both primers are shown in Fig. 1A). The corresponding wild-type controls are also shown in Fig. 1B (lanes 3 and 5). Table 1 depicts the single-knockout mutants we constructed.

Double knockouts. We also completed the construction of two double knockouts, *mutS ndk* and *mutY mutM* (Table 1). The procedure for making the double-knockout mutants was similar to the procedure used for making the single knockouts, except that the second gene in the double-knockout mutant (such as *ndk* or *mutM*, respectively) was replaced by an antibiotic resistance-encoding cassette that was different from the antibiotic resistance cassette, Ω-Sp, used to replace the first gene, as depicted in Fig. 2. We used Ω-Km, from the plasmid pUTE618, which confers kanamycin resistance (3; also T. Koehler, personal communication). The double-knockout mutants were identified as those colonies that were resistant to both spectinomycin and kanamycin but sensitive to erythromycin. The knockout mutations were further verified by PCR, demonstrating the loss of two wild-type genes and the presence of both Ω-Sp and Ω-Km. Together, these knockout strains were used for mutagenesis studies with *B. anthracis* and for further development of the *rpoB*/Rif^r system, as described below.

Measuring mutation frequencies and rates. We measured the Rif^r frequency in cultures grown in LB at 37°C and calculated the mutation rates per generation (see Materials and Methods), as described previously (see reference 9 and references therein). Table 2 shows the results for the wild type and for the knockout mutants that we constructed, including *mutY*, *mutM*, *mutS*, and *ndk*, as well as the double-knockout mutants *mutY mutM* and *mutS ndk*. It can be seen that whereas *mutM* and *mutY* strains are weak mutators by themselves, the combination of *mutY* and *mutM*, which lacks the ability to repair 8-oxoguanine, generates an enormous mutation rate per generation (μ) that is 269 times that of the wild type and results in frequencies in overnight cultures (approximately 30 generations) that are 1,000-fold higher than those of the wild type. Mutants that are *mutS* and lack mismatch repair have Rif^r frequencies 178-fold higher than the wild type in overnight cultures. Although *ndk* strains (with altered nucleoside triphosphate pools) show up as weak mutators, the combination of *mutS ndk* results in frequencies that are 786-fold higher than the wild type.

Use and extension of the *rpoB*/Rif^r system. Table 3 shows the distribution of spontaneous mutations in *rpoB* leading to the Rif^r phenotype; those from *mutS* strains, *mutY* strains, *mutY mutM* strains; and those occurring after treatment with the mutagens 5AZ and MNNG. (Note that the location numbers

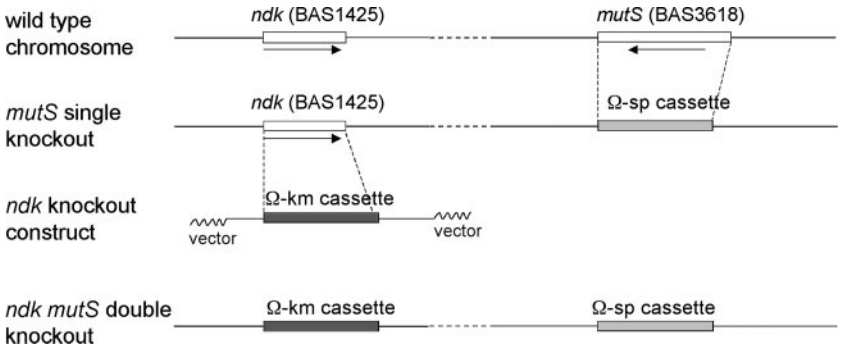

FIG. 2. Schematic representation of the targeting strategy for generating a *mutS ndk* double-knockout mutant. The *ndk*-coding region in the *mutS* single-knockout mutant was replaced by a kanamycin resistance-encoding cassette through reciprocal recombination to generate a *mutS ndk* double-knockout mutant. White boxes represent coding regions of *mutS* and *ndk*. Light gray boxes represent the spectinomycin resistance-encoding cassette. Dark gray boxes represent the kanamycin resistance-encoding cassette.

TABLE 3. Distribution of mutations leading to Rif^r in *B. anthracis*

B. anthracis site (bp)[a]	Amino acid change	Base pair change	No. of mutations							
			Spontaneous							
			This study	Total[b]	*mutS*	*mutS ndk*	*mutY*	*mutY mutM*	5AZ	MNNG
1403	Q454R	AT→GC	15	24‡	19	8	0	0	0	0
1442	H467R	AT→GC	17	23‡	20	10	0	0	0	2
1441	H467Y	GC→AT	20	23‡	1	0	0	0	0	31
1391	S450F	GC→AT	0	0	0	0	0	0	0	0
1457	S472F	GC→AT	1	4‡	0	0	0	0	0	8
1457*	S472Y	GC→TA	1	1	0	0	10	0	0	0
1402	Q454K	GC→TA	1	2‡	0	0	27	30	0	0
1403*†	Q454L	AT→TA	0	0	0	0	0	0	0	0
1417	T459S	AT→TA	0	0	0	0	0	0	0	0
1444	K468Q	AT→CG	0	0	0	0	0	0	0	0
1442*	H467P	AT→CG	1	1	0	0	0	0	0	0
1391	S450C	GC→CG	0	0	0	0	0	0	0	0
1441*	H467D	GC→CG	0	0	0	0	0	0	17	0
1400	S453C	GC→CG	0	0	0	0	0	0	0	0
Total (14)			56	78‡	40	18	37	30	17	41

[a] Symbols: *, new mutational changes in *B. anthracis* detected in this study; †, site detected after analysis of additional mutations from the same cultures (see Materials and Methods) as those included in the first column of spontaneous mutations.
[b] ‡, includes data from Vogler and coworkers (31).

for each base pair are 42 bp higher than previously reported 31). It can be seen that there are distinct hotspots for each mutator and for each mutagenic treatment. The spontaneous mutations are almost exclusively at 3 of the 14 sites detected in the *rpoB* gene so far. Previous work by Vogler and coworkers (31) detected 11 of these sites, and the work described here has resulted in three new sites being uncovered. The second column in the spontaneous category presents the totals when the spontaneous mutations found by Vogler and coworkers (31) are added to these. The *mutY* and *mutY mutM* strains have increased levels only of the G:C → T:A changes, while strains defective in *mutS* have increases mainly at the A:T → G:C sites. MNNG induces G:C → A:T changes; 5AZ induces only G:C → C:G changes and only at one site. These results are similar in form to those we found in the *rpoB* gene of *E. coli* (9). However, the frequency of Rif^r mutations, as first noted by Keim and coworkers, is an order of magnitude lower than that seen in *E. coli*. Is this because of an inherently lower mutation rate, or because of a distinctly lower number of mutational sites (14 so far in *B. anthracis rpoB* versus 77 in *E. coli rpoB*)? Some considerations in the following sections point to the latter explanation.

Comparisons of hotspots at different positions in *rpoB* in *B. anthracis* and in two other bacteria. Because of the high degree of sequence conservation in parts of the *rpoB* gene among prokaryotes, we can compare the DNA sequences surrounding

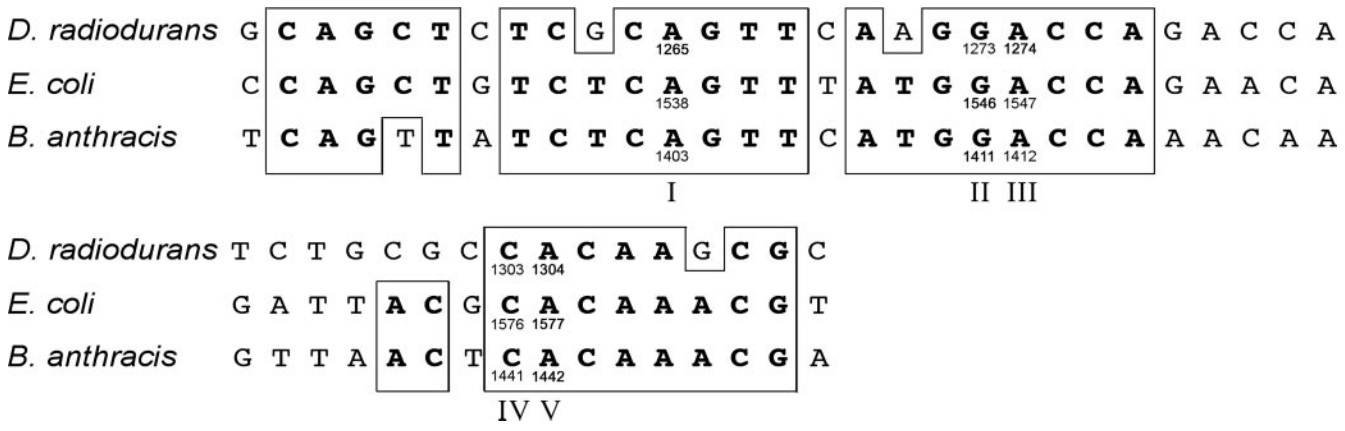

FIG. 3. DNA sequences surrounding specific sites in *rpoB*. Portions of the *rpoB* genes from *D. radiodurans*, *E. coli*, and *B. anthracis* are aligned. Five sites are designated by Roman numerals. Identical bases are indicated in boldface type. Mutation rates at these sites are given in Table 4.

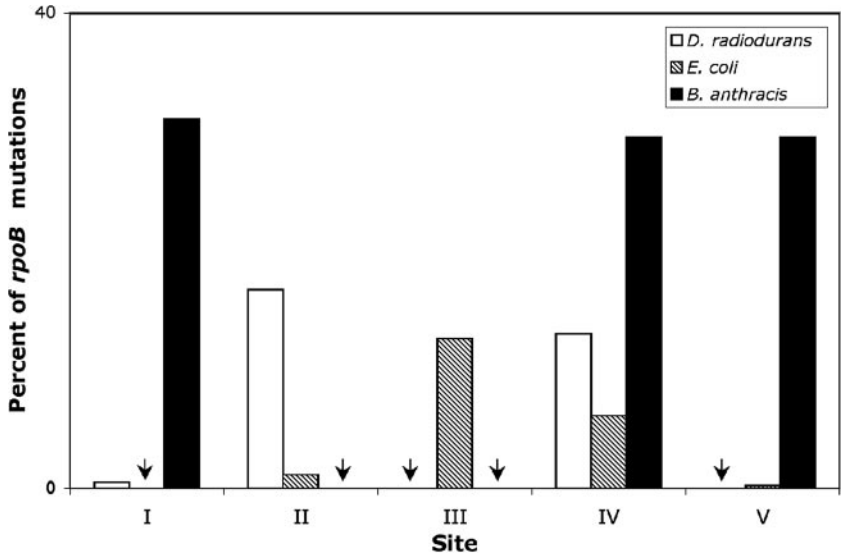

FIG. 4. Comparison of relative mutation frequencies observed at specific sites in *rpoB*. The values for five sites in *rpoB* in three different bacteria are shown as the percentage of all detected *rpoB* mutations that lead to Rif^r mutants. Arrows point to sites where no occurrences were detected. In some but not all cases, this is due to the failure of the mutation to generate a viable Rif^r mutant (see Table 4).

mutational sites in *rpoB* in several bacteria for which we have measured the mutation rates that lead to Rif^r. Figure 3 aligns the corresponding regions of *rpoB* near some of the most frequently mutated sites in *Deinococcus radiodurans* (14), *Escherichia coli* (9, 32), and *Bacillus anthracis* (31; also this work). Figure 4 displays the relative frequency among *rpoB* mutations in each organism for five selected sites (sites I to V in Fig. 3). Here, arrows depict sites at which no occurrences were detected. Despite extensive identities in surrounding sequences, there are dramatic differences in the relative mutation frequencies in the three bacteria. Table 4 converts these relative frequencies to actual mutation rates per site. (At site I, no occurrences were found in *E. coli* among 444 spontaneous mutations [32], although this site has been found in different mutator strains. The numbers in parentheses for this site represent 95% confidence limits.) Site I is the best example of a clear difference in mutation rates at the same base in a sequence context that is identical for the three or four nearest neighbors on each side, in the case of *B. anthracis* and *E. coli*, with only slightly less identity in the case of *D. radiodurans*. Site II also shows an apparent difference between *D. radiodurans* and *E. coli*, as does site V between *E. coli* and *B. anthracis*. The question of whether the failure to find mutations at sites II and III in *B. anthracis* and at sites III and V in *D. radiodurans* is due to very low mutagenicity (cold spots) or the failure of the respective base change to result in a rifampin-resistant phenotype requires additional experiments. We have done these in the case of *B. anthracis*, using site-directed mutagenesis (described below) to show that sites II and III do not yield the Rif^r phenotype when changed from G to A (site II) or A to G (site III).

TABLE 4. Mutation rates (μ) at sites in *rpoB*

rpoB site	μ (10^a)[a]		
	D. radiodurans	*E. coli*	*B. anthracis*
I	0.042 (1265)†	0–0.1* (1538)	0.49 (1403)
II	1.3 (1273)	0.17 (1546)	— (1411)
III	— (1274)	2.0 (1547)	— (1412)
IV	1.0 (1303)	0.91 (1576)	0.47‡ (1441)
V	— (1304)	0.034 (1577)	0.47 (1442)
Avg/site (total no. of sites)	0.19 (33)	0.19 (77)	0.11 (14)
Avg/transition site (total no. of transition sites)	0.31 (10)	0.23 (27)	0.29 (5)

[a] Data for *D. radiodurans* are from reference 14; data for *E. coli* are from reference 32. *, 95% confidence limit; ‡, GC→AT transition at this site; —, mutation rate cannot be determined at this site; †, base pair location.

Table 4 also shows the average mutation rate per site in *rpoB*, based on 33 sites in *D. radiodurans*, 77 in *E. coli*, and 14 in *B. anthracis*. *D. radiodurans* and *E. coli* display identical rates, whereas that of *B. anthracis* is almost twofold lower. Whether this apparent difference will hold when many more sites are considered remains to be seen. The vast majority of the spontaneous base substitutions in *rpoB* that lead to the Rif^r phenotype are transitions in *D. radiodurans* and *B. anthracis*, although to a lesser degree in *E. coli*. Therefore, we have charted at the bottom of Table 4 the average transition rate per site in the three bacteria. Keeping in mind that this average rate is based on fewer sites, we see that in all three cases they are within a range of from 2.3×10^{-10} to 3.1×10^{-10}. Here, the rates for *B. anthracis* are not lower than for *E. coli*.

Site-directed mutagenesis of the *B. anthracis rpoB* gene. The failure to find mutations in the *B. anthracis rpoB* gene, in cases where the corresponding location in *E. coli* or *D. radiodurans rpoB* is a hotspot, led us to ask whether mutations at these sites are rare in *B. anthracis* or simply do not lead to a viable Rif^r organism. We chose to construct two *rpoB* mutants, each of which contains a single-base substitution mutation at one of

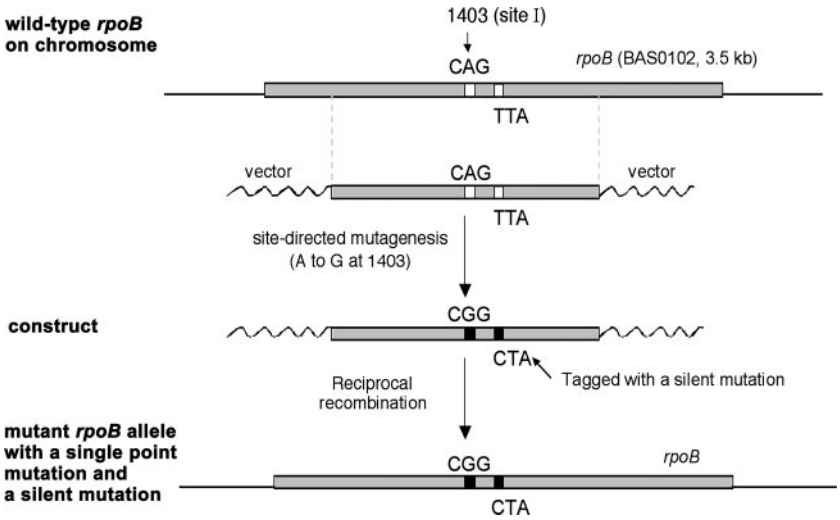

FIG. 5. Schematic representation of the strategy for generating a single point mutation in the *B. anthracis rpoB* gene. After cloning of a portion of the *rpoB* gene (~2 kb in length), a single point mutation (A→G at position 1403) was introduced into the coding region of the *rpoB* gene along with a tag (T→C at position 1426, a silent mutation) by using the QuickChange mutagenesis kit (Stratagene). The wild-type *rpoB* DNA sequence on the chromosome was replaced by the mutated DNA sequence through reciprocal recombination. Gray boxes represent a portion of the *rpoB* gene. White boxes represent the original codons (CAG and TTA) in the wild-type *rpoB* gene. Black boxes represent the mutated codons (CGG and CTA) in the *rpoB* mutant.

the following locations, G→A at position 1411 and A→G at position 1412, both of which have not yet been detected in *B. anthracis rpoB* mutants, although the corresponding positions in the *D. radiodurans* (G→A at position 1546) or *E. coli* (A→G at position 1547) *rpoB* gene are hotspots (see Fig. 3 and 4 and Table 4). We also decided to construct an additional *rpoB* mutant, A→G at position 1403, which naturally occurs among *B. anthracis rpoB* mutants, as a positive control.

The procedures for generating a single-base substitution in the *rpoB* gene are summarized as follows (Fig. 5). A DNA fragment of the *B. anthracis rpoB* gene (~2 kb in length, with the base pair targeted for the base substitution, e.g., A/T at position 1403, placed in the center) was subcloned into the cloning vector pCR2.1TOPO (Invitrogen). Then, a single-base substitution was introduced into the cloned *rpoB* gene fragment by site-directed mutagenesis using a QuickChange mutagenesis kit (Stratagene). In order to distinguish the base substitution we introduced from spontaneous occurrences of the same mutation, we also introduced a second silent point mutation, T→C at position 1426, that leads to TTA to CTA (both encode the amino acid residue leucine), as a tag. The *rpoB* gene fragment that contains the designed base substitution and the tag was subcloned into pUTE583 (Ery^r), the same shuttle vector that we used for constructing gene knockouts. The plasmid DNA was prepared from a Dam^- *E. coli* strain and electroporated into *B. anthracis* wild-type cells. The Ery^r transformants were selected and purified. The purified transformants were grown in the absence of antibiotic selection for several days to allow reciprocal recombination and subsequent loss of the shuttle vector. The colonies that were resistant to rifampin but sensitive to erythromycin were further studied.

We analyzed the frequency of Rif^r and determined the nature of the base substitution mutations in the *rpoB* gene among those Rif^r colonies (which also lost the shuttle vector). The results are shown in Table 5. The Rif^r frequency for the positive control (A→G at position 1403), a naturally occurring site, was 10×10^{-9}. Note that this frequency is generated by site-directed mutagenesis and is thus different from that for spontaneously occurring mutations. Among 19 Rif^r colonies analyzed, all except 1 contained both A→G 1403 and the tag CTA, demonstrating that the procedure for making the site-directed *rpoB* mutation on the *B. anthracis* chromosome worked. The Rif^r frequencies of the other two base substitution samples (intended for G→A at position 1411 and A→G at position 1412) are 0.4×10^{-9} and 0.5×10^{-9}, respectively, which is about 20- to 25-fold lower than the Rif^r frequency obtained from the positive control and even somewhat below the background spontaneous mutation frequency (see Table 2). Moreover, among 16 Rif^r colonies analyzed, none of them contain the mutation we intended to introduce. Our results very strongly indicate that the specific base substitutions we

TABLE 5. Site-directed mutagenesis of the *rpoB* gene on the *B. anthracis* chromosome

Intended base substitution	Rif^r frequency (10^9) (95% confidence limit)	No. of correct base substitutions/ total no. of substitutions	Adjusted Rif^r frequency (10^9) (95% confidence limit)
A→G at 1403 (naturally occurring site)	10 (8.0–12.9)	18/19	9.5 (7.6–12.2)
G→A at 1411 (not yet detected)	0.4 (0–0.8)	0/8	0.03 (0–0.15)
A→G at 1412 (not yet detected)	0.5 (0–0.6)	0/8	0.03 (0–0.15)

made at positions 1411 and 1412 on the *B. anthracis rpoB* gene do not lead to Rif^r in *B. anthracis*.

DISCUSSION

Recent advances in developing methods for recombinant shuttle vectors, for generating gene knockouts, and for using transposon mutagenesis in *Bacillus anthracis* (2, 3, 16, 26, 29; also T. Koehler, personal communication), as well as the knowledge of the complete *B. anthracis* genome sequence (25), now make it feasible to begin a serious program aimed at fully characterizing in vivo mutational pathways, mutational avoidance pathways, and DNA repair in this important microorganism. There is surprisingly little variation among *B. anthracis* isolates (13), but Keim and coworkers have used rare single-nucleotide polymorphisms and variable-number tandem repeats to develop forensic analyses crucial to aiding law enforcement and national security (13). Understanding the forces behind this low but visible diversity can only aid in continued refinement of forensic studies.

In this work, we created mutator strains by constructing the following knockout mutants: *mutS*, *mutY*, *mutM*, *ndk*, and the double knockouts *mutY mutM* and *mutS ndk*. Each corresponding mutant of *E. coli* displays a specific base substitution spectrum in the *rpoB* gene (reference 9 and unpublished data). We therefore utilized the *rpoB* gene of *B. anthracis*. The RNA polymerase β subunit, and particularly that portion involved in rifampin binding, is highly conserved in prokaryotes (22), and mutations conferring Rif^r have been found in numerous microorganisms; in most cases, these affect positions in the protein corresponding to those found in *E. coli* (see references 9, 22, and 31 and references therein). We have developed an extensive *rpoB*/Rif^r mutation analysis system for both *Escherichia coli* (9, 32) and *Deinococcus radiodurans* (14). Fortunately, Vogler and coworkers have carried out a pilot study with *B. anthracis* and have shown that Rif^r mutants of this organism indeed result from mutations at expected sites in the *rpoB* gene (31). They analyzed 22 spontaneous and 23 UV-induced mutations in an attenuated *B. anthracis* strain and found that they fell into 10 mutational sites, all within a small cluster, making them amenable to PCR amplification and sequencing with a single primer pair in each case. We have already extended this analysis here, using the *B. anthracis* Sterne 7702 strain, increasing the number of sites to 14.

We measured mutation rates in *B. anthracis* and compared the specificity of mutations with those seen in the *rpoB* gene in *E. coli* and in some cases in *Deinococcus radiodurans* (14). We supplemented this work by analyzing mutations generated with 5AZ and MNNG. The mutation rates for each mutator are depicted in Table 2. The increases relative to the wild type follow the same pattern as seen with *E. coli* (1, 9, 17, 20, 21, 23). Thus, mutators that are either *mutM* or *mutY* give small increases, whereas the double mutant *mutY mutM* gives very large increases. Strains that are *mutS* are strong mutators, and *ndk* results in a weak mutator, although it does enhance the effect of *mutS* when part of a *mutS ndk* double mutant. In all cases, the frequencies and rates are 5- to 20-fold lower than the corresponding values for *E. coli.* Moreover, we find that the *rpoB* spontaneous mutation rate in *B. anthracis* (1.6×10^{-9} per replication) is 10-fold lower than we measured for *E. coli* (20). Vogler and coworkers (31) first reported the *rpoB* rate in *B. anthracis*, by a different method, and also found it to be 1.6×10^{-9} per replication. We can show that this apparent lower level of mutagenesis, which is 10-fold less than that for *E. coli rpoB*, is primarily a result of fewer sites in *rpoB* that can mutate to yield viable rifampin-resistant colonies (14 found so far compared with almost 80 in *E. coli*). Table 4 compares the average rate per site in *rpoB* for *E. coli*, *D. radiodurans*, and *B. anthracis*, based on 77, 33, and 14 sites, respectively. These rates vary only from 1.1×10^{-10} per replication for *B. anthracis* to 1.9×10^{-10} per replication for both *E. coli* and *D. radiodurans*. Moreover, the average transition rate varies from 2.3×10^{-10} to 3.1×10^{-10} per replication, with that of *B. anthracis* slightly higher than that of *E. coli.* Interestingly, as Fig. 3 and 4 and Table 4 show, the same sites can have widely varying mutation rates in each of the three organisms, even when the surrounding base sequence is identical. For example sites I and V show 10-fold (or more)-higher rates of mutation in *B. anthracis* than in *E. coli*, despite very similar surrounding sequences, particularly for site I. Thus, hotspots are highly species specific and reflect interactions of polymerase, editing, and repair proteins with the mutational site and surrounding sequences. Each protein has its own inherent specificity with regard to sites and surrounding sequences.

Comparative genomics suggests the presence of auxiliary repair pathways for *B. anthracis* when we compare the *B. anthracis* genome with the *B. subtilis* genome in the category of DNA replication, recombination, and repair (see the introduction). Furthermore, when we compare the *B. anthracis* genome with the *E. coli* K-12 genome in the same gene category (http://www.ncbi.nlm.nih.gov/sutils/cogtik.cgi?gi=115&cog=L), we find that 17 COGs in *B. anthracis*, some with multiple orthologs, are absent from *E. coli* and 15 COGs in *B. anthracis* contain additional protein members (data not shown). *B. anthracis* appears to have additional DNA repair capabilities for UV-induced DNA damage (25) and several proteins that have detoxification functions (25). Investigations of their roles in mutation avoidance will be the subject of future studies.

ACKNOWLEDGMENTS

We thank Ken Bradley and Theresa Koehler for bacterial strains and plasmids and together with Paul Keim for helpful advice.

This work was supported by a grant from the National Institutes of Health (ES010875).

REFERENCES

1. **M. Cabrera, Y. Nghiem, and J. H. Miller.** 1988. *mutM*, a second mutator locus in *Escherichia coli* that generates GC Æ TA transversions. J. Bacteriol. **170:**5405–5407.
2. **Cendrowski, S., W. MacArthur, and P. Hanna.** 2004. *Bacillus anthracis* requires siderophore biosynthesis for growth in macrophages and mouse virulence. Molec. Microbiol. **51:**407–417.
3. **Chen, Y., F. C. Tenover, and T. M. Koehler.** 2004. β-lactamase gene expression in a penicillin-resistant *Bacillus anthracis* strain. Antimicrobial Agents and Chemotherapy **48:**4873–4877.
4. **Dai, Z., C. Sirard, M. Mock, and T. M. Koehler.** 1995. The *atxA* gene product activates transcription of the anthrax toxin genes and is essential for virulence. Mol. Micriobiol. **16:**1171–1181.
5. **De Groote, M. A., U. A. Ochsner, M. U. Shiloh, C. Nathan, J. McCord, M. C. Dinauer, S. J. Libby, A. Vazquez-Torres, Y. Xu, and F. C. Fang.** 1997. Periplasmic superoxide dismutase protects Salmonella from products of phagocyte NADPH-oxidase and nitric oxide synthase. Proc. Natl. Acad. Sci. USA **94:**13997–14001.
6. **Dixon, W. J., and F. J. Massey, Jr.** 1969. Introduction to statistical analysis. McGraw-Hill, New York, NY.

7. **Drake, J. W.** 1991. a constant rate of spontaneous mutation in DNA-based microbes. Proc. Natl. Acad. Sci. USA **88:**7160–7164.
8. **Friedberg, E. C., G. C. Walker, W. Seide, R. D. Wood, R. A. Schultz, and T. Ellenberger.** 2006. DNA Repair and Mutagenesis, Am. Soc. Microbiol., Washington, DC.
9. **Garibyan, L., T. Huang, M. Kim, E. Wolff, A. Nguyen, T. Nguyen, A. Diep, K. Hu, A. Iverson, H. Yang, and J. H. Miller.** 2003. Use of the *rpoB* Gene to Determine the Specificity of Base Substitution Mutations on the *Escherichia coli* Chromosome. DNA Repair. **2:**593–608.
10. **Green, B. D., L. Battisti, T. M. Koehler, and C. B. Thorne.** 1985. Demonstration of a capsule plasmid in *Bacillus anthracis.* Infect. Immun. **49:**291–297.
11. **Guidi-Rontani, C., Y. Periera, S. Ruffie, J. C. Sirard, M. Weber-Levy, and M. Mock.** 1999. Identification and characterization of the germination operon on the virulence plasmid pXO1 of *Bacillus anthracis.* Mol. Microbiol. **33:** 407–414.
12. **Keim, P., L. B. Price, A. M. Klevytska, K. L. Smith, J. M. Schupp, R. Okinaka, P. J. Jackson, and M. E. Hugh-Jones.** 2000. Multiple-locus variable-number tandem repeat analysis reveals genetic relationships within *Bacillus anthracis.* J. Bacteriol. **182:**2928–2936.
13. **Keim, P., M. N. Van Ert, T. Pearson, A. J. Vogler, L. Y. Huhn, and D. M. Wagner.** 2004. Anthrax molecular epidemiology and forensics: using the appropriate marker for different evolutionary scales. Infect. Genet. & Evolution. **4:**205–213.
14. **Kim, M., E. Wolff, T. Huang, L. Garibyan, A. M. Earl, J. R. Battista, and J. H. Miller.** 2004. Developing a genetic system in *Deinococcus radiodurans* for analyzing mutations. Genetics **166:**661–668.
15. **Koehler, T. M.** 2002. *Bacillus anthracis* genetics and virulence gene regulation. Curr. Top. Microbiol. Immunol. **271:**143–164.
16. **Koehler, T. M., Z. Dai, and M. Kaufman-Yarbray.** 1994. Regulation of the *Bacillus anthracis* protective antigen gene: CO_2 and a *trans*-acting element activate transcription from one of the two promoters. J. Bacteriol. **175:**586–595.
17. **Michaels, M. L., C. Cruz, A. P. Grollman, and J. H. Miller.** 1992. Evidence that MutM and MutY combine to prevent mutations by an oxidatively damaged form of guanine in DNA. Proc. Natl. Acad. Sci. USA **89:**7022–7025.
18. **Miller, J. H.** 1992. A short course in bacterial genetics: A laboratory manual and handbook for *Escherichia coli* and related bacteria. Cold Spring Harbor Laboratory Press, Cold Spring Harbor, NY.
19. **Miller, J. H.** 2005. Perspective on mutagenesis and repair: The standard model and alternate modes of mutagenesis. Critical Rev. Biochem. Mol. Biol. **40:**155–179.
20. **Miller, J. H., P. Funchain, W. Clendenin, T. Huang, A. Nguyen, E. Wolff, A. Yeung, J. Chiang, L. Garibyan, M. M. Slupska, and H. Yang.** 2002. *Escherichia coli* strains (*ndk*) lacking nucleoside diphosphate kinase are powerful mutators for base substitutions and frameshifts in mismatch repair deficient strains. Genetics **162:**5–13.
21. **Modrich, P.** 1991. Mechanisms and biological effects of mismatch repair. Annu. Rev. Genet. **25:**229–253.
22. **Musser, J. M.** 1995. Antimicrobial resistance in mycobacteria: molecular genetic insights. Clin. Microbiol. Rev. **8:**496–514.
23. **Nghiem, Y., M. Cabrera, C. G. Cupples, and J. H. Miller.** 1988. The *mutY* gene: a mutator locus in *Escherichia coli* that generates GC → TA transversions. Proc. Natl. Acad. Sci. USA **85:**2709–2713.
24. **Okinaka, R. T., K. Cloud, O. Hampton, A. R. Hoffmaster, K. K. Hill, P. Keim, T. M. Koehler, G. Lamke, S. Kumano, J. Mahillon, D. Manter, Y. Martinex, D. Ricke, R. Svensson, and P. J. Jackson.** 1999. Sequence and organization of pXO1, the large *Bacillus anthracis* plasmid harboring the anthrax toxin genes. J. Bacterial. **18:**6509–6515.
25. **Read, T. D., S. N. Peterson, N. Tourasse, L. W. Baillie, I. Paulsen, K. E. Nelsen, H. Tettelin, D. E. Fouts, J. A. Eisen, S. R. Gill, E. K. Holtzapple, O. A. Okstad, E. Helgason, J. Rilstone, M. Wu, J. F. Kolonay, M. J. Beanan, R. J. Dodson, L. M. Brinkac, M. Gwinn, R. T. DeBoy, R. Madpu, S. C. Daugherty, A. S. Durkin, D. H. Haft, W. C. Nelson, J. D. Petersen, M. Pop, H. M. Khouri, D. Radune, J. L. Benton, Y. Mahamoud, L. Jiang, I. R. Hance, J. F. Weidman, K. J. Berry, R. D. Plaut, A. M. Wolf, K. L. Watkins, W. C. Nierman, A. Hazen, R. Cline, C. Redmond, J. E. Thwaite, O. White, S. L. Salzberg, B. Thomason, A. M. Friedlander, T. M. Koehler, P. C. Hanna, A.-B. Kolsto, and C. Fraser.** 2003. The genome sequence of *Bacillus anthracis* Ames and comparison to closely related bacteria. Nature **423:**81–86.
26. **Saile, E., and T. M. Koehler.** 2002. Control of anthrax toxin gene expression by the transition state regulator *abrB.* J. Bacteriol. **184:**370–380.
27. **Setlow, P.** 1995. Mechanisms for prevention of damage to DNA in spores of Bacillus species. Annu. Rev. Microbiol. **49:**29–54.
28. **Smith, B. T., A. D. Grossman, and G. C. Walker.** 2002. Localization of UvrA and effect of DNA damage on the chromosome of *Bacillus subtilis.* J. Bacteriol. **184:**488–493.
29. **Tinsley, E., A. Naqvi, A. Bourgogne, T. M. Koehler, and S. A. Khan.** 2004. Isolation of a minireplicon of the virulence plasmid pXO2 of *Bacillus anthracis* and characterization of the plasmid-encoded RepS replication protein. J. Bacteriol. **186:**2717–2723.
30. **Uchida, I., S. Makino, T. Sekizaki, and N. Terakado.** 1997. Identification of a novel gene, dep, associated with depolymerization of the capsular polymer in *Bacillus anthracis.* Mol. Microbiol. **9:**487–496.
31. **Vogler, A. J., J. D. Busch, S. Percy-Fine, C. Tipton-Hunton, K. L. Smith, and P. Keim.** 2002. Molecular Analysis of rifampicin resistance in *Bacillus anthracis* and *Bacillus cereus.* Antimicrob. Agents and Chemo. **46:**511–513.
32. **Wolff, E., M. Kim, K. Hu, H. Yang, and J. H. Miller.** 2004. Polymerases leave fingerprints: analysis of the mutational spectrum in *Escherichia coli rpoB* to assess the role of polymerase IV in spontaneous mutation. J. Bacteriol. **186:**2900–2905.